Sodankylä, Finland

# **FALCON**™ Airborne Gravity Gradiometer Survey

for

**Anglo American Exploration B.V. Suomen Sivuliike**

# Processing Report

Survey Flown: August, 2011

By

**FUGRO AIRBORNE SURVEYS Pty Ltd**
U3/435 Scarborough Beach Rd
Osborne Park, WA, 6017
AUSTRALIA

FASP Job# 2244
FASO Job# 11809

# TABLE OF CONTENTS

## FIGURES

## TABLES

# 1 INTRODUCTION

Fugro Airborne Surveys conducted a high-sensitivity aeromagnetic and **FALCON**™ Airborne Gravity Gradiometer (AGG) survey over the Mosku-Sakatti survey area under contract with Anglo American Exploration B.V Suomen Sivuliike.

## 1.1 Survey Location

The Mosku-Sakatti survey area is centred on longitude 26°38' E, latitude 67º 35' N (see the location map in Figure 1).

The production flights took place during August 2011 with the first production flight taking place on August 11th and the final flight taking place on August 12th. To complete the survey area coverage a total of 4 production flights were flown, for a combined total of 1751 line kilometres of data acquired.

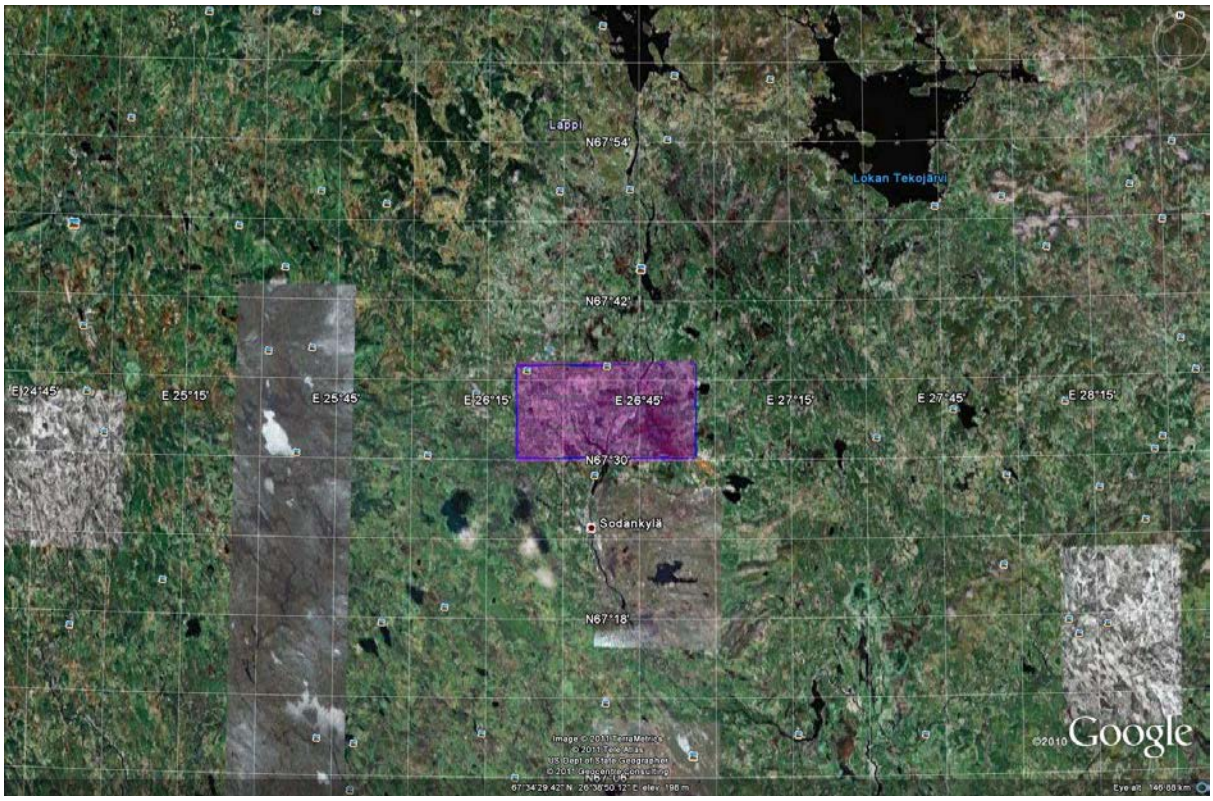


**Figure 1: Mosku-Sakatti –** *Survey Area Location*

# 2 SUMMARY OF SURVEY PARAMETERS

## 2.1 Survey Area Specifications

**Mosku-Sakatti**

| | |
|---|---|
| Total Kilometres (km) | 1751 |
| Nominal Terrain Clearance (m) | 80 |
| Clearance Method | Radar |
| Traverse Line Direction (deg.) | 090 / 270 |
| Traverse Line Spacing (m) | 200 |
| Tie Line Direction (deg.) | 000 / 180 |
| Tie Line Spacing (m) | 4250 |

The survey block is defined by the coordinates in Table 1, in KKJ Finnish Uniform Coordinate System.

| Corner Number | Easting | Northing |
|---|---|---|
| 1 | 3472298 | 7503604 |
| 2 | 3497417 | 7503604 |
| 3 | 3497417 | 7490658 |
| 4 | 3472298 | 7490658 |

**Table 1: Mosku-Sakatti –** *Survey Boundary Coordinates*

## 2.2 Data Recording

The following parameters were recorded during the course of the survey:

- **FALCON™ AGG data**: recorded at different intervals.
- **Airborne total magnetic field**: recorded with a 0.1 s sampling rate.
- **Aircraft altitude**: measured by the barometric altimeter at intervals of 0.1 s.
- **Terrain clearance**: provided by the radar altimeter at intervals of 0.1 s.
- **Airborne GPS positional data**: (latitude, longitude, height, time and raw range from each satellite being tracked): recorded at intervals of 1 s.
- **Time markers**: in digital data.
- **Ground total magnetic field**: recorded with a 1 s sampling rate.
- **Ground based GPS positional data**: (latitude, longitude, height, time and raw range from each satellite being tracked): recorded at intervals of 1 s.
- **Aircraft distance to ground**: measured by the laser scanner system, scanning at 20 times per second (when in range of the instrument and in the absence of thick vegetation).

## 2.3 Job Safety Plan, HSE Summary

A Job Safety Plan and Job Safety Analysis was prepared and implemented in accordance with the Fugro Airborne Surveys Occupational Safety and Health Management System.

# 3 FIELD OPERATIONS

## 3.1 Operations

The survey was based out of Sodankylä, Finland. The survey aircraft was operated from Sodankylä airport using aircraft fuel available on site. A temporary office was set up in Sodankylä where all survey operations were run and the post-flight data verification was performed.

## 3.2 Base Stations

A dual frequency GPS base station was set up at the airport in order to correct the raw GPS data collected in the aircraft. A secondary GPS base station was available, but was not required.

**GPS Base Station**

| | |
|---|---|
| Date: | August 3rd, 2011 |
| Location: | Sodankylä airport |
| Latitude: | 67º 23' 44.0926" N |
| Longitude: | 26º 36' 53.4596" E |
| Height: | 203.075 m ellipsoidal |

**Magnetometer Base Station (CF1)**

| | |
|---|---|
| Location: | Sodankylä airport |
| Base: | 53015 nT |

## 3.3 Field Personnel

The following technical personnel participated in field operations:

| | |
|---|---|
| Crew Leader: | D. MacDonald |
| Pilots: | S. Cowan and D. Wiens |
| Technician: | D. MacDonald |
| Project Manager: | D. Grenier |
| Final QC and Processing: | W. Irvine and E. Rooen |

# 4 QUALITY CONTROL RESULTS

## 4.1 Survey acquisition issues

During the course of the survey there were no data quality issues with:

AGG instrumentation
Mag and GPS base stations
Airborne magnetometer system
Data acquisition systems
Radar altimeter
Laser scanner

## 4.2 Flight Path Map

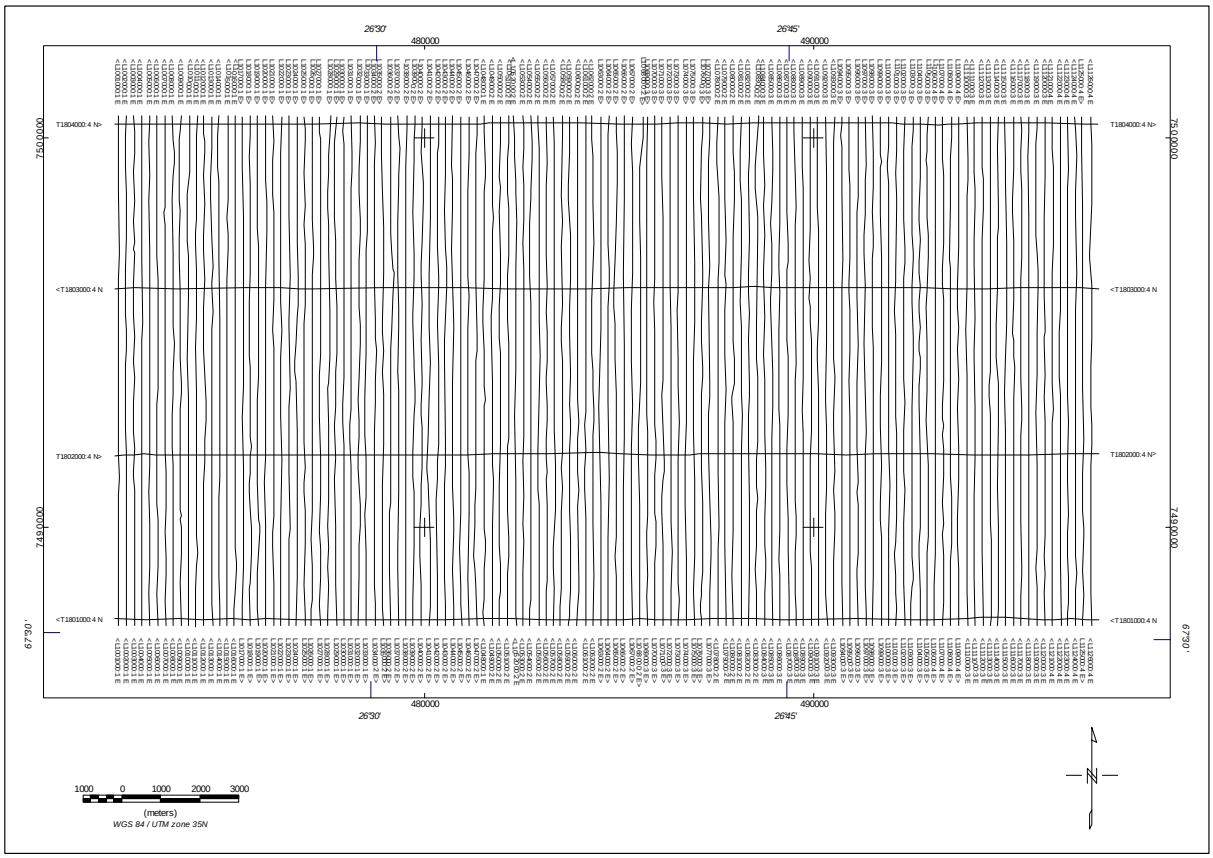


**Figure 2: Mosku-Sakatti –** *Flight Path map*

## 4.3 Turbulence

The mean turbulence recorded in the Mosku-Sakatti survey area was 54.4 milli g (where g = 9.80665 m/sec/sec). Turbulence was fairly uniform and ranged from moderate to high. The turbulence pattern across the survey area is shown in Figure 3.

**Figure 3: Mosku-Sakatti –** *Turbulence (milli g where g = 9.80665 m/sec/sec)*

## 4.4 AGG System Noise

The system noise is defined to be the standard deviation of half the difference between the A & B complements, for each of the NE and UV curvature components. The results for this survey were very good with values of 3.01 E and 3.10 E for NE and UV respectively.

Figure 4 and Figure 5 provide a representation of the variation in this standard deviation for each component. This is achieved by gridding a rolling measurement of standard deviation along each line using a window length of 100 data points.

**Figure 4: Mosku-Sakatti –** *System Noise NE (*E*)*

**Figure 5: Mosku-Sakatti –** *System Noise UV (E)*

## 4.5 Digital Terrain Model

Laser scanner range data were combined with GPS position and height data (adjusted from height above the WGS84 ellipsoid to height above the geoid by applying the Earth Gravitational Model 1996 (EGM96)). The output of this process is a "swath" of terrain elevations extending either side of the aircraft flight path. Width and sample density of this swath varies with aircraft height. Typical values are 100 to 150 metres and 5 to 10 metres respectively.

Because terrain correction of AGG data requires knowledge of the terrain at distances up to at least 10 km from the data location, laser scanner data collected only along the survey line path must be supplemented by data from another source. For this purpose, Shuttle Radar Topography Mission (SRTM) v2 data are usually chosen. For this survey in the absence of available SRTM data, client supplied regional DTM data were used.

Laser scanner data quality was good with scan density generally above 90%. Laser scanner data were gridded at 10 m with a 1 cell maximum extension beyond data limits. The gaps were then filled using a Fourier domain data wrapping approach. To supplement the laser data, regional DTM data were excised to an area 15 km beyond the survey area. The excised data were filled using the same Fourier domain wrapping method, then adjusted to the level of the laser scanner data prior to merging.

Figure 6 shows the final Digital Terrain Model resulting from the laser scanner and regional DTM data processing.

**Figure 6: Mosku-Sakatti –** *Final Digital Terrain Model (metres above WGS84 ellipsoid with EGM96 geoid correction)*

## 4.6 Terrain Clearance

Terrain clearance for the Mosku-Sakatti survey averaged slightly above the nominal clearance of 80 m having a mean value of 88.4 m across the survey area. The terrain clearance, as derived from laser scanner data, is shown in Figure 7.

**Figure 7: Mosku-Sakatti –** *Terrain Clearance from laser scanner data (metres above ground surface)*

# 5 FALCON™ AIRBORNE GRAVITY GRADIENT (AGG) RESULTS

## 5.1 Processing Summary

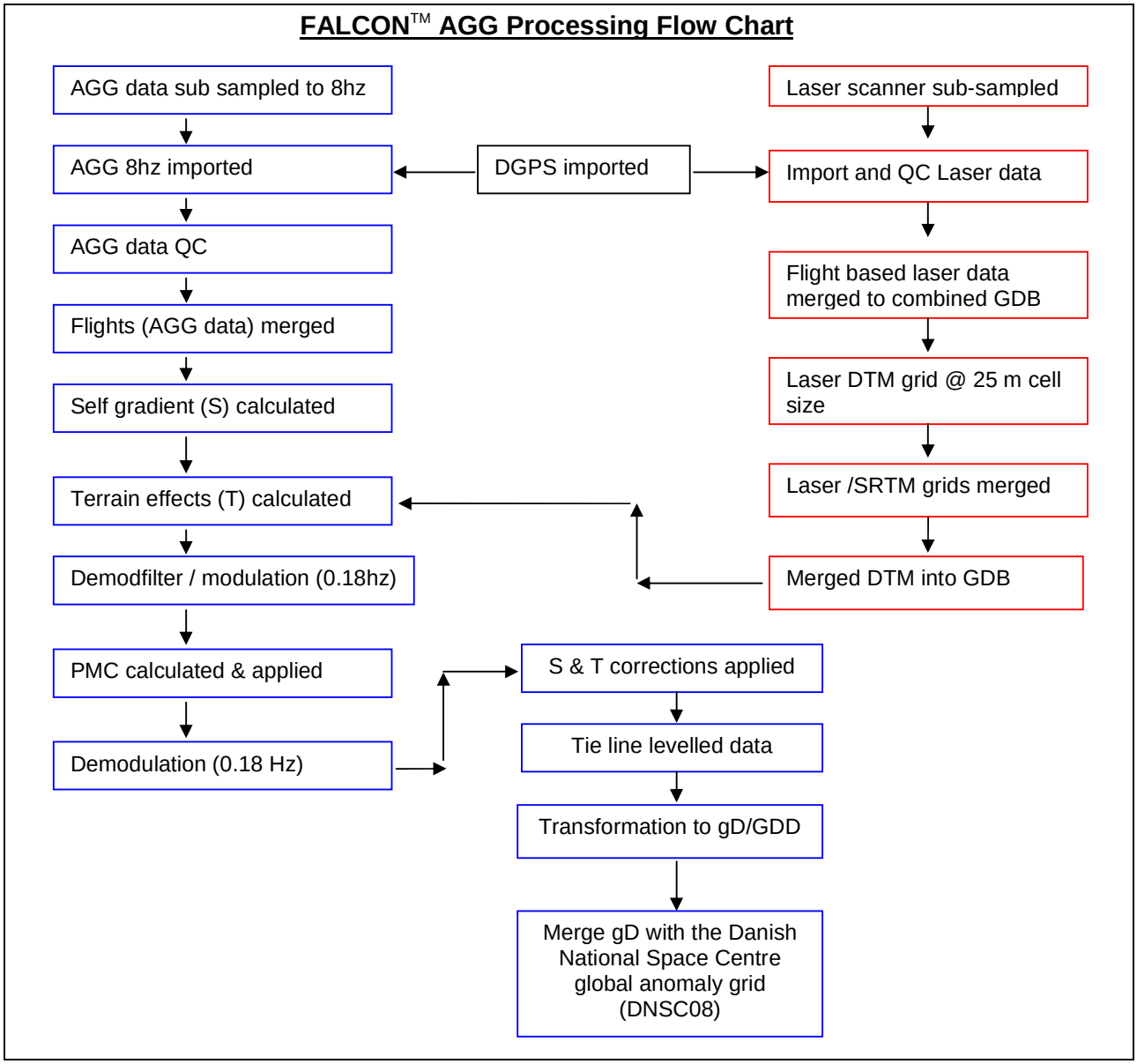


**Figure 8:** *FALCON™ AGG Data Processing*

## 5.2 FALCON™ Airborne Gravity Gradiometer Data

Figure 8 summarises the steps involved in processing the AGG data obtained from the survey.

The **FALCON**™ Airborne Gravity Gradiometer data were digitally recorded by the ADAS on removable hard drives. The raw data were then copied on to the field processing laptop, backed up twice onto DVD+R media and shipped to Fugro Perth using a secure courier service.

Preliminary processing and QC of the **FALCON™** AGG data were completed on-site using Fugro's DiAGG software.
Further QC and Final **FALCON™** AGG data processing were performed by the office based data processor.

## 5.3 Radar Altimeter Data

The terrain clearance measured by the radar altimeter in metres was recorded at 10 Hz. The data were plotted and inspected for quality.

## 5.4 Laser Scanner Data

The terrain clearance measured by the laser scanner in metres was recorded at 20 scans/sec with 276 data points per scan, and was then sub-sampled using a window width of 0.25 sec. The sub-sampled laser scanner data were edited for spikes prior to gridding.

## 5.5 Positional Data

A number of programs were executed for the compilation of navigation data in order to reformat and recalculate positions in differential mode. Waypoint's GrafNav GPS processing software was used to calculate DGPS positions from raw range data obtained from the moving (airborne) and stationary (ground) receivers.

The GPS ground station position was determined by logging GPS data continuously for 24 hours prior to survey flights commencing. The GPS data were processed and quality controlled completely in the field.

Positional data (longitude, latitude, Z) were output in the WGS84 datum. The longitude and latitude data were then projected into UTM Zone 35N coordinates. All processing was performed using WGS84/UTM Zone 35N coordinates. Final line data were supplied in this projection in addition to the KKJ/Finnish Uniform Coordinate System. Final grid data were supplied using KKJ/Finnish Uniform Coordinate System coordinates.

Parameters for the KKJ datum are:

| | |
|---|---|
| Ellipsoid: | International 1924 |
| Semi-major axis: | 6378388 m |
| 1/flattening: | 297 |

## 5.6 Additional Processing

For the terrain correction, in the absence of any knowledge of the local geology, the standard density of 2.67 g/cc was selected. Typically 2.67 g/cc will work well for most terrain types but may lead to over correction or under correction in some areas. The data were tie line levelled.

## 5.7 FALCON™ Airborne Gravity Gradient Data - $G_{DD}$ & $g_D$

The transformation into $G_{DD}$ and $g_D$ was accomplished using two methods: Fourier domain transformation and the Method of Equivalent Sources

### Fourier

The Fourier domain transformation method uses a low-pass filter to improve the signal to noise ratio by removing processing artefacts and other information which is known to be beyond the sampling resolution. A cut-off wavelength of 200 m was used in the low-pass filter.

### Equivalent Source

The equivalent source transformation utilises a smooth model inversion to calculate the density of a surface of sources followed by a forward calculation to produce $g_D$ and $G_{DD}$. It was possible to closely match the wavelength characteristics of the Fourier results by placing the sources at a depth of 200 metres.

### Drape Surfaces

Both transformations use a smoothed surface onto which the output data are projected. These surfaces are smoother equivalents of the actual flying surface.

The Fourier and Equivalent Source $G_{DD}$ (density 2.67 g/cc) maps are shown in Figure 9 and Figure 10 respectively.

Two versions of vertical gravity ($g_D$) are presented: Fourier, derived by integrating the $G_{DD}$; and Equivalent Source, derived directly from the modelled sources. The (density 2.67 g/cc) Fourier result is presented in Figure 11 and the (density 2.67 g/cc) Equivalent Source result is presented in Figure 12.

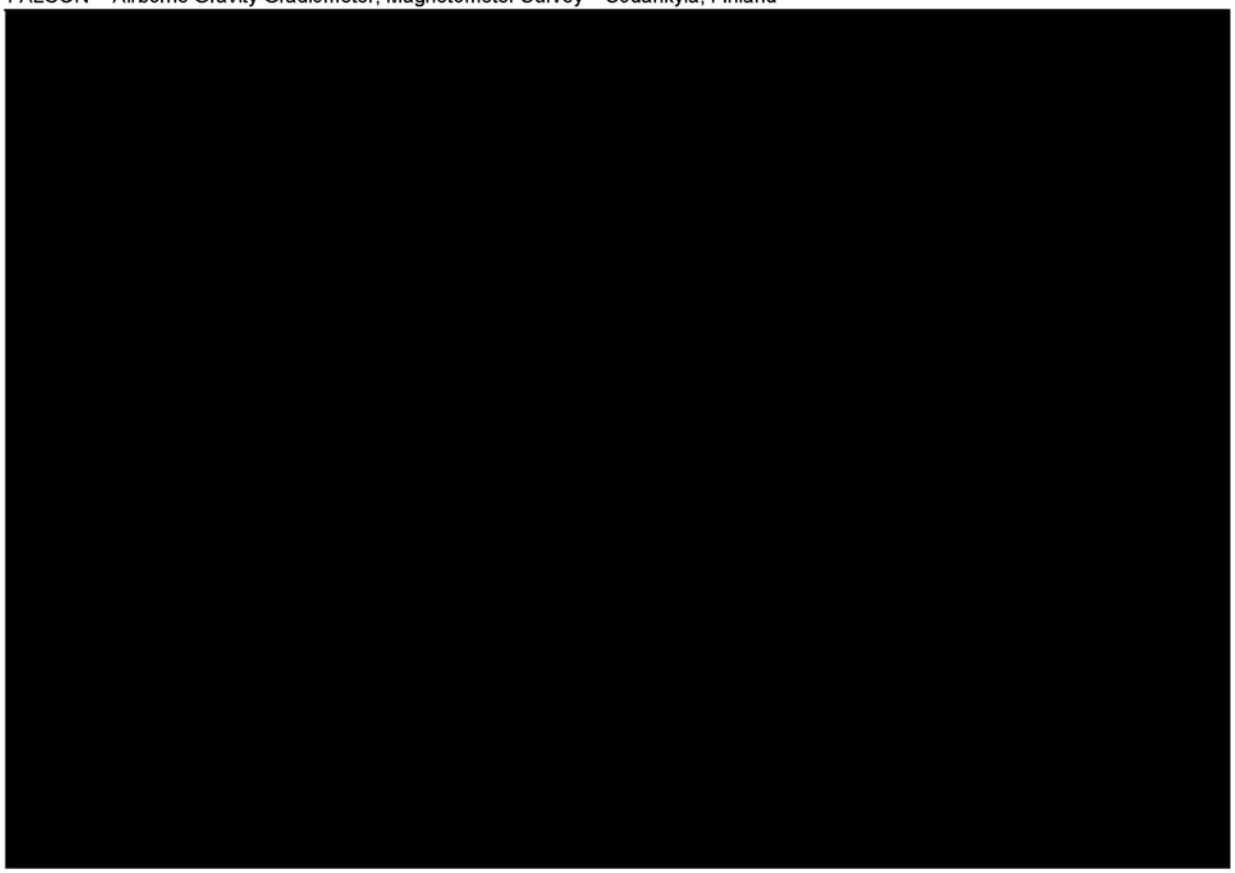

**Figure 9: Mosku-Sakatti –** *Vertical Gravity Gradient ($G_{DD}$) from Fourier processing (E).*

**Figure 10: Mosku-Sakatti –** *Vertical Gravity Gradient ($G_{DD}$) from Equivalent Source processing (E).*

**Figure 11: Mosku-Sakatti –** *Vertical Gravity ($g_D$) from Fourier processing (mGal)*

## 5.8 Conforming $g_D$ to regional gravity

As discussed in section 9.3, the long wavelength information in $g_D$ (both the Fourier and Equivalent Source versions) can be improved by incorporating ancillary information. Such information is available in the form of the global anomaly grid compiled by the Danish National Space Centre (DNSC08).

The Fourier and Equivalent Source gD grids were conformed to a grid derived from the DMSC08 data as follows.

- Low pass filter the regional data using a cosine squared filter with cut-off at 30km, tapering to 20km.
- High pass filter the $g_D$ data (Fourier and Equivalent Source) using a cosine squared filter with cut-off at 30 km, tapering to 20km.
- Conform the Fourier and Equivalent Source data to the regional data by addition of the filtered grids. The filter design is such that this method provides uniform frequency response across the overlap frequencies.

Further discussion of this method can be found in Dransfield (2009).

The (density 2.67 g/cc) results are presented in Figure 13 and Figure 14.

# 6 AEROMAGNETIC RESULTS

## 6.1 Processing Summary

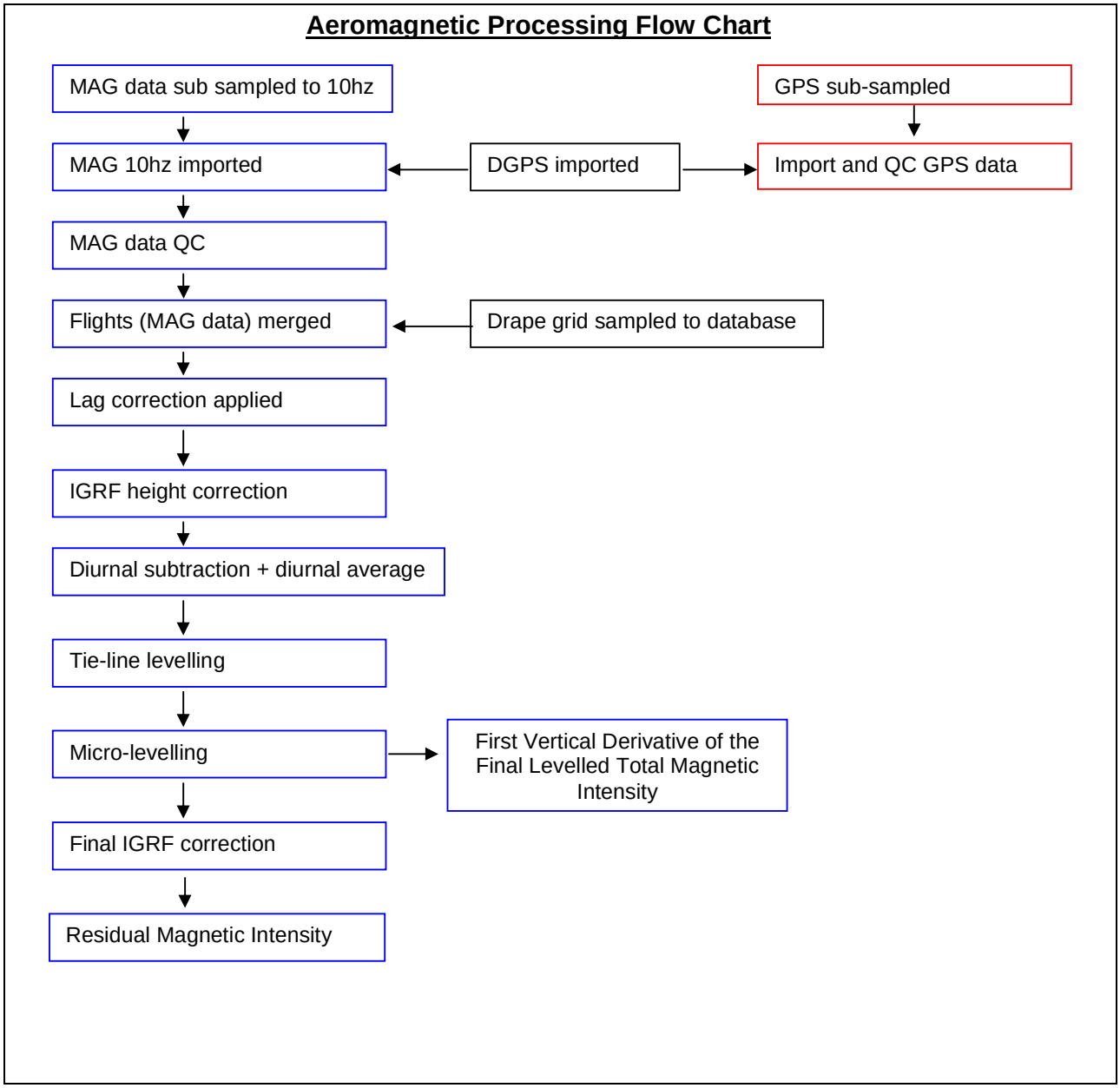


**Figure 15:** *Aeromagnetic Data Processing*

## 6.2 Aeromagnetic Data

Figure 15 summarises the steps involved in processing the aeromagnetic data obtained from the survey.

The aeromagnetic data were digitally recorded by the FASDAS on removable hard drives. The raw data were then copied onto the field processing laptop, backed up twice onto hard drive media and sent via FTP to Fugro's secure server.

Preliminary QC of the aeromagnetic data was completed on-site using Fugro's proprietary

ATLAS software.

Further QC and aeromagnetic data processing were performed by the office based data processor.

### 6.3 Radar Altimeter Data

The terrain clearance measured by the radar altimeter in metres was recorded at 10 Hz. The data were plotted and inspected for quality.

### 6.4 Positional Data

A number of programs were executed for the compilation of navigation data in order to reformat and recalculate positions in differential mode. Waypoint's GrafNav GPS processing software was used to calculate DGPS positions from raw range data obtained from the moving (airborne) and stationary (ground) receivers.

The GPS ground station position was determined by logging GPS data continuously for 24 hours prior to survey flights commencing. The GPS data were processed and quality controlled completely in the field.

Positional data (longitude, latitude, Z) were output in the WGS84 datum. The longitude and latitude data were then projected into UTM Zone 35N coordinates. All processing was performed using WGS84/UTM Zone 35N coordinates. Final line data were supplied in this projection in addition to the KKJ/Finnish Uniform Coordinate System. Final grid data were supplied using KKJ/Finnish Uniform Coordinate System coordinates.

Parameters for the KKJ datum are:

| | |
|---|---|
| Ellipsoid: | International 1924 |
| Semi-major axis: | 6378388 m |
| 1/flattening: | 297 |

### 6.5 Lag Correction

All aeromagnetic data were lagged prior to final processing. A lag of 0.35 seconds was applied

### 6.6 IGRF Height Correction

The IGRF was calculated using the drape height and using the GPS height to produce a height corrected total magnetic intensity. A final IGRF correction was applied during a later step.

### 6.7 Diurnal Subtraction

The base station magnetics (diurnal) were filtered using a long wavelength filter to retain wavelengths longer than 71 seconds. This value was subtracted from the height corrected total magnetic intensity. Next, based upon the average magnetic value calculated from running the base station for 24 hours, a base value of 53015 nT was added back to the magnetics. This produced the diurnally corrected total magnetic intensity.

## 6.8 Tie-line Levelling

At this stage the total magnetic intensity data were tie-line levelled using Fugro's proprietary ATLAS software.

## 6.9 Micro-levelling

At this stage the total magnetic intensity data were micro-levelled using Fugro's proprietary ATLAS software.

## 6.10 Total Magnetic Intensity

The total magnetic intensity had a minimum value of 51949 nT and a maximum value of 61972 nT across the survey area presented in Figure 16.

## 6.11 First Vertical Derivative of the Total Magnetic Intensity

The first vertical derivative of the total magnetic intensity had a minimum value of -13.3407 nT/m and a maximum value of 50.7729 nT/m across the survey area presented in Figure 17.

## 6.12 Final IGRF Correction

The levelled total magnetic intensity was then IGRF corrected using the 2010 model, 2011/08/15 as the removal date and a constant elevation of 310 m above the WGS84 ellipsoid. The output from this correction is the residual magnetic intensity.

## 6.13 Residual Magnetic Intensity

The residual magnetic intensity had a minimum value of -1395 nT and a maximum value of 8734 nT across the survey areas.

# 7 APPENDIX I - SURVEY EQUIPMENT

## 7.1 Survey Aircraft

A Fugro Airborne Surveys Cessna C208B turbo prop, Canadian registration C-GGRD (Newton), was used to fly the survey area. The following instrumentation was used for this survey.

## 7.2 FALCON™ Airborne Gravity Gradiometer

**FALCON**™ *AGG System*
The **FALCON**™ AGG System is based on current state-of-the-art airborne gravity gradiometer technology and has been optimized for airborne broad band geophysical exploration. The system is capable of supporting surveying activities in areas ranging from 1,000 ft below sea level to 13,000 ft above sea level with aircraft speeds from 70 to 130 knots. The **FALCON**™ AGG data streams were digitally recorded at different rates on removable drives installed in the **FALCON**™ AGG electronics rack.

## 7.3 Airborne Data Acquisition Systems

*Fugro Digital Acquisition System (FASDAS)*
The Fugro FASDAS is a data acquisition system executing propriety software for the acquisition and recording of location, magnetic and ancillary data. Data are presented both numerically and graphically in real time on the VGA display providing on-line quality control capability.

The FASDAS is also used for real time navigation. A pre-programmed flight plan containing boundary coordinates, line start and end coordinates, the altitude values calculated for a theoretical drape surface, line spacing and cross track definitions is loaded into the computer prior to each flight. The WGS-84 latitude and longitude and altitude received from the real-time corrected, dual frequency Novatel OEMV L1/l2-Band Positioning receiver, is transformed to the local coordinate system for cross track and distance to go values. This information, together with ground heading and speed, is displayed to the pilot numerically and graphically on a two line LCD display. It is also presented on the operator LCD screen in conjunction with a pictorial representation of the survey area, survey lines and ongoing flight path.

**FALCON**™ *AGG Data Acquisition System (ADAS)*
The Fugro DAS provides control and data display for the **FALCON**™ AGG system. Data are displayed real time for the operator and warnings displayed should system parameters deviate from tolerance specifications. All **FALCON**™ AGG and laser scanner data are recorded to a removable hard drive.

## 7.4 Aerial and Ground Magnetometers

The airborne Caesium magnetometer was a Scintrex CS-3 having a noise envelope of 0.002nT pk-pk in 0.01-1Hz bandwidth. The ground magnetometer was a Scintrex CS3 Caesium sensor sampling at 1Hz.

## 7.5 Real-Time Differential GPS

*Novatel OEMV L-Band Positioning*
The Novatel OEMV L-band Positioning receiver provides real-time differential GPS for the onboard navigation system. The differential data set was relayed via a geo-synchronous satellite to the aircraft where the receiver optimized the corrections for the current location.

## 7.6 GPS Base Station Receiver

*Novatel OEM4 L1/L2*
The Novatel GPS receiver is a 12 channel dual frequency GPS receiver. It provides raw range information of all satellites in view sampled every second and recorded on a computer laptop. This data are post-processed with the rover data to provide differential GPS (DGPS) corrections for the flight path.

## 7.7 Altimeters

*King KRA405 Radar Altimeter*
*Fugro Digital Barometric Pressure Sensor*
The radar altimeter has a resolution of 1m, an accuracy of 2%, a range of 1-2,500 ft and a measurement rate of 10 Hz. The barometric pressure is measured with an on board pressure module (Rosemount 1241M) with a suitable pneumatic connection to a Pitot-static system.

## 7.8 Laser Scanner

*Riegl LMS-Q140I-80*
The laser scanner is designed for high speed line scanning applications. The system is based upon the principle of time-of-flight measurement of short laser pulses in the infrared wavelength region and the angular deflection of the laser beam is obtained by a rotating polygon mirror wheel. The measurement range is up to 400 m with a minimum range of 2 m and an accuracy of 50mm. The laser beam is eye safe, the laser wavelength is 0.9 μm, the scan angle range is +/- 40° and the scan speed is 20 scans/s.

## 7.9 Data Processing Hardware and Software

The following equipment and software were used:

**Hardware**
- One 2.0 GHz (or higher) laptop computer
- External USB hard drive reader for ADAS removable drives
- Two External USB hard drives for data backup
- HP DeskJet All-In-One printer, copier, scanner

**Software**
- Oasis Montaj data processing and imaging software
- GrafNav Differential GPS processing software
- Fugro - Atlas data processing software
- Fugro - DiAGG Processing software

# 8 APPENDIX II - SYSTEM TESTS

## 8.1 Instrumentation Lag

Due to the relative position of the magnetometer, altimeters and GPS antenna on the aircraft and to processing/recording time lags, raw readings from each data stream vary in position. To correct for this and to align selected anomaly features on lines flown in opposite directions, the magnetic and altimeter data are 'parallaxed' with respect to the position information. The lags were applied to the data during processing.

## 8.2 Radar Altimeter Calibration

The radar altimeter is checked for accuracy and linearity every 12 months, or when any change in a key system component requires this procedure to be carried out. This calibration allows the radar altimeter data to be compared and assessed with the other height data (GPS, barometric and laser) to confirm the accuracy of the radar altimeter over its operating range. The calibration is performed by flying a number of 30 second lines at preselected terrain clearances over an area of flat terrain and using the results of the radar altimeter, differentially corrected GPS heights in mean sea level (MSL) and laser scanner were used to derive slope and offset information.

## 8.3 FALCON™ AGG Noise Measurement

At the commencement of the survey, 20 minutes of data were collected with the aircraft in straight level flight at 3500 ft AGL. These data were processed as a survey line to check the AGG noise levels.

Daily flight debriefs incorporating FALCON™ AGG performance statistics for each flight line are prepared using output from Fugro DiAGG software. These are sent daily to Fugro office staff for performance evaluation.

## 8.4 Daily Calibrations

A set of daily calibrations were performed each survey day as follows:
- Magnetic base station time check
- AGG Quiescent Calibration

### 8.4.1 Magnetic Base Station Time Check

Prior to each day's survey all magnetic base stations were synchronised using broadcast GPS time signals.

### 8.4.2 FALCON™ AGG Calibration

A calibration was performed at the beginning of each flight and the results monitored by the operator. The coefficients obtained from each of the calibrations were used in the processing of the data.

# 9 APPENDIX III - FALCON™ AGG DATA & PROCESSING

## 9.1 Nomenclature

The Falcon airborne gravity gradiometer (AGG) system adopts a North, East, and Down coordinate sign convention and these directions (N, E, and D) are used as subscripts to identify the gravity gradient tensor components (gravity vector derivatives). Lower case is used to identify the components of the gravity field and upper case to identify the gravity gradient tensor components. Thus the parameter usually measured in a normal exploration ground gravity survey is $\mathbf{g_D}$ and the vertical gradient of this component is $\mathbf{G_{DD}}$.

## 9.2 Units

The vertical component of gravity ($\mathbf{g_D}$) is delivered in the usual units of mGal. The gradient tensor components are delivered in eotvos, which is usually abbreviated to "E". By definition **$1\ E = 10^{-4}$ mGal/m.**

## 9.3 FALCON Airborne Gravity Gradiometer Surveys

In standard ground gravity surveys, the component measured is "$\mathbf{g_D}$", which is the *vertical component of the acceleration due to gravity*. In airborne gravity systems, since the aircraft is itself accelerating, measurement of "$\mathbf{g_D}$" cannot be made to the same precision and accuracy as on the ground. Airborne gravity gradiometry uses a differential measurement to remove the aircraft motion effects and delivers gravity data of a spatial resolution and sensitivity comparable with ground gravity data.

The Falcon gradiometer instrument acquires two curvature components of the gravity gradient tensor namely $\mathbf{G_{NE}}$ and $\mathbf{G_{UV}}$ where $\mathbf{G_{UV}} = (\mathbf{G_{EE}} - \mathbf{G_{NN}})/2$. Since these curvature components cannot easily and intuitively be related to the causative geology, they are transformed into the vertical gravity gradient ($\mathbf{G_{DD}}$), and integrated to derive the vertical component of gravity ($\mathbf{g_D}$). Interpreters display, interpret and model both $\mathbf{G_{DD}}$ and $\mathbf{g_D}$. The directly measured $\mathbf{G_{NE}}$ and $\mathbf{G_{UV}}$ data are appropriate for use in inversion software to generate density models of the earth. The vertical gravity gradient, $\mathbf{G_{DD}}$, is more sensitive to small or shallow sources and has greater spatial resolution than $\mathbf{g_D}$ (similar to the way that the vertical magnetic gradient provides greater spatial resolution and increased sensitivity to shallow sources of the magnetic field). In the integration of $\mathbf{G_{DD}}$ to give $\mathbf{g_D}$, the very long wavelength component, at wavelengths comparable to or greater than the size of the survey area, cannot be fully recovered. Long wavelength gravity are therefore incorporated in the $\mathbf{g_D}$ data from other sources. This might be regional ground, airborne or marine gravity if such data are available. The Danish National Space Centre global gravity data of 2008 (DNSC08) are used as a default if other data are not available.

## 9.4 Gravity Data Processing

The main elements and sequence of processing of the gravity data are as follows:

1. Dynamic corrections for residual aircraft motion (called Post Mission Compensation or PMC) are calculated and applied.
2. Self gradient corrections are calculated and applied to reduce the time-varying gradient response from the aircraft and platform.
3. A Digital Terrain Model (DTM) is created from the laser scanner range data, the AGG inertial navigation system rotation data and the DGPS position data.
4. Terrain corrections are calculated and applied.

5. $\mathbf{G_{NE}}$ and $\mathbf{G_{UV}}$ are levelled and transformed into the full gravity gradient tensor, including $\mathbf{G_{DD}}$, and into $\mathbf{g_D}$.

## 9.5 Aircraft dynamic corrections

The design and operation of the FALCON AGG results in very considerable reduction of the effects of aircraft acceleration but residual levels are still significant and further reduction is required and must be done in post-processing.

Post-processing correction relies on monitoring the inertial acceleration environment of the gravity gradiometer instrument (GGI) and constructing a model of the response of the GGI to this environment. Parameters of the model are adjusted by regression to match the sensitivity of the GGI during data acquisition. The modelled GGI output in response to the inertial sensitivities is subtracted from the observed output. Application of this technique to the output of the GGI, when it is adequately compensated by its internal mechanisms, reduces the effect of aircraft motion to acceptable levels.

Following these corrections, the gradient data are demodulated and filtered along line with a 6-pole Butterworth low-pass filter with a cut-off frequency of 0.18 Hz (for fixed-wing operations; a higher frequency may be used for helicopter operations).

## 9.6 Self gradient Corrections

The GGI is mounted in gimbals controlled by an inertial navigation system which keeps the GGI pointing in a fixed direction whilst the aircraft and gimbals rotate around it. Consequently, the GGI measures a time-varying gravity gradient due to these masses moving around it as the heading and attitude of the aircraft changes during flight. This is called the self-gradient.

Like the aircraft dynamic corrections, the self-gradient is calculated by regression of model parameters against measured data. In this case, the rotations of the gimbals are the input variables of the model. Once calculated, the modelled output is subtracted from the observed output.

## 9.7 Laser Scanner Processing

The laser scanner measures the range from the aircraft to the ground in a swathe of angular width ±40 degrees below the aircraft. The aircraft attitude (roll, pitch and heading) data provided by the AGG inertial navigation system are used to adjust the range data for changes in attitude and the processed differential GPS data are used to reference the range data to located ground elevations referenced to the WGS 84 datum. Statistical filtering strategies are used to remove anomalous elevations due to foliage or built up environment. The resulting elevations are gridded to form a digital terrain model (DTM).

## 9.8 Terrain Corrections

An observation point above a hill has excess mass beneath it compared to an observation point above a valley. Since gravity is directly proportional to the product of the masses, uncorrected gravity data have a high correlation with topography.

It is therefore necessary to apply a terrain correction to gravity survey data. For airborne gravity gradiometry at low survey heights, a detailed DTM is required. Typically,

immediately below the aircraft, the digital terrain will need to be sampled at a cell size roughly one-third to one-half of the survey height and with a position accuracy of better than 1 metre. For these accuracies, LIDAR data are required and each FALCON survey aircraft comes equipped with LIDAR (laser scanner).

If bathymetric data are used then these form a separate terrain model for which terrain corrections are calculated at a density chosen to suit the water bottom – water interface. Once the DTM has been merged, the terrain corrections for each of the $\mathbf{G_{NE}}$ and $\mathbf{G_{UV}}$ data streams are calculated. In the calculation of terrain corrections, a density of 1 gm/cc is used. The calculated corrections are stored in the database allowing the use of any desired terrain correction density by subtracting the product of desired density and correction from the measured $\mathbf{G_{NE}}$ and $\mathbf{G_{UV}}$ data. The terrain correction density is chosen to be representative of the terrain density over the survey area. Sometimes more than one density is used with input from the client.

Typically, the terrain corrections are calculated over a distance 10 km from each survey measurement point.

### 9.9 Tie-line Levelling

The terrain- and Self gradient-corrected $\mathbf{G_{NE}}$ and $\mathbf{G_{UV}}$ data are tie-line levelled across the entire survey using a least-squares minimisation of differences at survey line intersections. Occasionally some micro-levelling might be performed.

### 9.10 Transformation into $G_{DD}$ & $g_D$

The transformation of the measured, corrected and levelled $\mathbf{G_{NE}}$ and $\mathbf{G_{UV}}$ data into gravity and components of the full gravity gradient tensor is accomplished using two methods:

- Fourier domain transformation and
- Equivalent source transformation.

The Fourier method relies on the Fourier transform of Laplace's equation. The application of this transform to the complex function $\mathbf{G_{NE} + i\, G_{UV}}$ provides a stable and accurate calculation of each of the full tensor components and gravity. The Fourier method performs piece-wise upward and downward continuation to work with data collected on a surface that varies from a flat horizontal plane. For stability of the downward continuation, the data are low-pass filtered. The cut-off wavelength of this filter depends on the variations in altitude and the line spacing. It is set to the smallest value that provides stable downward continuation.

The equivalent source method relies on a smooth model inversion to calculate the density of a surface of sources and from these sources, a forward calculation provides the $\mathbf{G_{DD}}$ and $\mathbf{g_D}$ data. The smoothing results in an output that is equivalent to the result of the low-pass filter in the Fourier domain method.

The Fourier method generates all tensor components but the equivalent source method only generates $\mathbf{G_{DD}}$ and $\mathbf{g_D}$ (and $\mathbf{G_{NE}}$ and $\mathbf{G_{UV}}$ for comparison with the inputs).

The limitations of gravity gradiometry in reconstructing the long wavelengths of gravity can lead to differences in the results of these two methods at long wavelength. The merging of the $\mathbf{g_D}$ data with externally supplied regional gravity such as the DNSC08 gravity removes these differences.

## 9.11 Noise & Signal

With all the Falcon AGG instruments, there are two measurements made of both the NE and UV curvature components during acquisition. This gives a pair of independent readings at each sample point.

The standard deviation of half the difference between these pairs is a good estimate of the survey noise. This is calculated for each line, and the average of all the survey lines is the figure quoted for the survey as a whole.

This difference error has been demonstrated to follow a 'normal' or Gaussian statistical distribution, with a mean of zero. Therefore, the bulk of the population (95%) will lie between -2σ and +2σ of the mean. For a typical survey noise estimate of, say, 3 E, 95% of the noise will be between -6 E and +6 E.

These typical errors in the curvature gradients translate to errors in $\mathbf{G_{DD}}$ of about 5 E and in $\mathbf{g_D}$ (in the shorter wavelengths) in the order of 0.1 mGal.

## 9.12 Risk Criteria in Interpretation

The risks associated with a Falcon AGG survey are mainly controlled by the following factors.

- **Survey edge anomalies** – the transformation from measured curvature gradients to vertical gradient and vertical gravity gradient is subject to edge effects. Hence any anomalies located within about 2 x line spacing of the edge of the survey boundaries should be treated with caution.
- **Single line anomalies** – for a wide-spaced survey, an anomaly may be present on only one line. Although it might be a genuine anomaly, the interpreter should note that no two-dimensional control can be applied.
- **Low amplitude (less than 2σ) anomalies** – Are within the noise envelope and need to be treated with caution, if they are single line anomalies and close in diameter to the cut-off wavelengths used.
- **Residual topographic error anomalies** – Inaccurate topographic correction either due to inaccurate DTM or local terrain density variations may produce anomalies. Comparing the DTM with the $G_{DD}$ map terrain-corrected for different densities is a reliable way to confirm the legitimacy of an anomaly.
- **The low density of water and lake sediments** (if present) can create significant gravity and gravity gradient lows which may be unrelated to bedrock geology. It is recommended that all anomalies located within lakes or under water be treated with caution and assessed with bathymetry if available.

## 9.13 References

Boggs, D. B. and Dransfield, M. H., 2004, Analysis of errors in gravity derived from the Falcon airborne gravity gradiometer, Lane, R. (ed.), Airborne Gravity 2004 - Abstracts from the ASEG-PESA Airborne Gravity 2004 Workshop, Geoscience Australia Record 2004/18, 135-141.

Dransfield, M. H., 2009, Conforming FALCON gravity and the global gravity anomaly, Geophysical Prospecting, DOI: 10.1111/j.1365-2478.2009.00830.x

Dransfield, M. H. and Lee, J. B., 2004, The FALCON airborne gravity gradiometer survey systems, Lane, R. (ed.), Airborne Gravity 2004 - Abstracts from the ASEG-PESA Airborne Gravity 2004 Workshop, Geoscience Australia Record 2004/18, 15-19.

Dransfield, M. H. and Zeng, Y., Airborne gravity gradiometry: terrain corrections and elevation error, *submitted to Geophysics*.

Lee, J. B., 2001, FALCON Gravity Gradiometer Technology, Exploration Geophysics, 32, 75-79.

Lee, J. B.; Liu, G.; Rose, M.; Dransfield, M.; Mahanta, A.; Christensen, A. and Stone, P., 2001, High resolution gravity surveys from a fixed wing aircraft, Geoscience and Remote Sensing Symposium, 2001. IGARSS '01. IEEE 2001 International, 3, 1327-1331.

Stone, P. M. and Simsky, A., 2001, Constructing high resolution DEMs from Airborne Laser Scanner Data, Preview, Extended Abstracts: ASEG 15th Geophysical Conference and Exhibition, August 2001, Brisbane, 93, 99.

# 10 APPENDIX IV - FINAL PRODUCTS

Final FALCON™ AGG digital line data were provided in an 8 Hz ASCII and Geosoft Oasis GDB database files containing the fields and format described in Table 2 below.

Final aeromagnetic digital line data were provided in a 10Hz ASCII and Geosoft Oasis GDB database files containing the fields and format described in Table 3 below.

Grids of all Fourier and Equivalent Source products, Gravity Gradient Tensors, Total Magnetic Intensity, First Vertical Derivative of the Total Magnetic Intensity, as well as the DTM were delivered as described in Table 4 below. The grids are in Geosoft GRD and ERMapper ERS formats with a 50 m cell size, with the exception of the DTM grid which has a 10 m cell size.

One copy of the digital archives was delivered along with a hard copy of this Logistics and Processing Report.

| Field | Variable | Description | Units |
|---|---|---|---|
| 1 | line | Line Number | - |
| 2 | time_1980 | Universal Time (Seconds Since January 6, 1980) | seconds |
| 3 | flight | Flight Number | - |
| 4 | date | Date of Survey Flight | yyyymmdd |
| 5 | lat_kkj | Latitude in KKJ | degrees |
| 6 | long_kkj | Longitude in KKJ | degrees |
| 7 | lat_wgs84 | Latitude in WGS84 | degrees |
| 8 | long_wgs84 | Longitude in WGS84 | degrees |
| 9 | x_kkj | Easting (X) in KKJ Finland Uniform Coordinate System | metres |
| 10 | y_kkj | Northing (Y) in KKJ Finland Uniform Coordinate System | metres |
| 11 | x_wgs84 | Easting (X) in WGS84 UTM Zone 35N | metres |
| 12 | y_wgs84 | Northing (Y) in WGS84 UTM Zone 35N | metres |
| 13 | gpsz | GPS Elevation (Referenced to Mean Sea Level) | metres |
| 14 | alt_radar | Radar Altimeter | metres |
| 15 | height | Calculated Laser Scanner Clearance (gpsz - dtm) | metres |
| 16 | dtm | Terrain (Referenced to Mean Sea Level) | metres |
| 17 | turbulence | Estimated vertical platform turbulence (vertical acceleration where g = 9.80665 m/sec/sec) | millig |
| 18 | Err_NE | NE gradient uncorrelated noise estimate, after tie-line levelling | eötvös |
| 19 | Err_UV | UV gradient uncorrelated noise estimate, after tie-line levelling | eötvös |
| 20 | T_DD | Terrain effect calculated for DD using a density of 1g/cc | eötvös |
| 21 | T_NE | Terrain effect calculated for NE using a density of 1g/cc | eötvös |
| 22 | T_UV | Terrain effect calculated for UV using a density of 1g/cc | eötvös |
| 23 | A_SJT_0_NE | Self gradient, jitter corrected NE gradient, no terrain correction | eötvös |
| 24 | A_SJT_0_UV | Self gradient, jitter corrected UV gradient, no terrain correction | eötvös |
| 25 | B_SJT_0_NE | Self gradient, jitter corrected NE gradient, no terrain correction | eötvös |
| 26 | B_SJT_0_UV | Self gradient, jitter corrected UV gradient, no terrain correction | eötvös |
| 27 | A_SJT_2p67_NE | Self gradient, jitter & terrain corrected NE gradient, terrain correction density 2.67 g/cc | eötvös |

| | | | |
|---|---|---|---|
| 28 | A_SJT_2p67_UV | Self gradient, jitter & terrain corrected UV gradient, terrain correction density 2.67 g/cc | eötvös |
| 29 | B_SJT_2p67_NE | Self gradient, jitter & terrain corrected NE gradient, terrain correction density 2.67 g/cc | eötvös |
| 30 | B_SJT_2p67_UV | Self gradient, jitter & terrain corrected UV gradient, terrain correction density 2.67 g/cc | eötvös |
| 31 | gD_Fourier_2p67 | Fourier derived vertical gravity, terrain correction density 2.67 g/cc, 200m cutoff wavelength | mGal |
| 32 | GEE_Fourier_2p67 | Fourier derived Gee gradient, terrain correction density 2.67 g/cc, 200m cutoff wavelength | eötvös |
| 33 | GNN_Fourier_2p67 | Fourier derived Gnn gradient, terrain correction density 2.67 g/cc, 200m cutoff wavelength | eötvös |
| 34 | GDD_Fourier_2p67 | Fourier derived vertical gravity gradient, terrain correction density 2.67 g/cc, 200m cutoff wavelength | eötvös |
| 35 | GED_Fourier_2p67 | Fourier derived Ged horizontal EW gradient, terrain correction density 2.67 g/cc, 200m cutoff wavelength | eötvös |
| 36 | GND_Fourier_2p67 | Fourier derived Gnd horizontal NS gradient, terrain correction density 2.67 g/cc, 200m cutoff wavelength | eötvös |
| 37 | GNE_Fourier_2p67 | Fourier derived Gne curvature gradient, terrain correction density 2.67 g/cc, 200m cutoff wavelength | eötvös |
| 38 | GUV_Fourier_2p67 | Fourier derived Guv curvature gradient, terrain correction density 2.67 g/cc, 200m cutoff wavelength | eötvös |
| 39 | Drapesurface_Fourier | Drape surface for Fourier reconstruction, smoothed flight surface | metres |
| 40 | gD_Fourier_0p0 | Fourier derived vertical gravity, no terrain correction applied, 200m cutoff wavelength | mGal |
| 41 | GEE_Fourier_0p0 | Fourier derived Gee gradient, no terrain correction applied, 200m cutoff wavelength | eötvös |
| 42 | GNN_Fourier_0p0 | Fourier derived Gnn gradient, no terrain correction applied, 200m cutoff wavelength | eötvös |
| 43 | GDD_Fourier_0p0 | Fourier derived vertical gravity gradient, no terrain correction applied, 200m cutoff wavelength | eötvös |
| 44 | GED_Fourier_0p0 | Fourier derived Ged horizontal EW gradient, no terrain correction applied, 200m cutoff wavelength | eötvös |
| 45 | GND_Fourier_0p0 | Fourier derived Gnd horizontal NS gradient, no terrain correction applied, 200m cutoff wavelength | eötvös |
| 46 | GNE_Fourier_0p0 | Fourier derived Gne curvature gradient, no terrain correction applied, 200m cutoff wavelength | eötvös |
| 47 | GUV_Fourier_0p0 | Fourier derived Guv curvature gradient, no terrain correction applied, 200m cutoff wavelength | eötvös |
| 48 | gD_Equiv_2p67 | Equivalent source derived vertical gravity, terrain correction density 2.67 g/cc | mGal |
| 49 | GDD_Equiv_2p67 | Equivalent source derived vertical gravity gradient, terrain correction density 2.67 g/cc | eötvös |
| 50 | GNE_Equiv_2p67 | Equivalent source derived Gne curvature gradient, terrain correction density 2.67 g/cc | eötvös |
| 51 | GUV_Equiv_2p67 | Equivalent source derived Guv curvature gradient, terrain correction density 2.67 g/cc | eötvös |
| 52 | Drapesurface_Equiv | Drape surface for Equivalent Source construction, approximates Fourier drape surface | metres |

**Table 2: Final FALCON™ AGG Digital Data** – *ASCII and Geosoft Database Format*

| Field | Variable | Description | Units |
|---|---|---|---|
| 1 | line | Line Number | - |
| 2 | time | Universal Time (Seconds Since Midnight) | seconds |
| 3 | time_1980 | Universal Time (Seconds Since January 6, 1980) | seconds |
| 4 | flight | Flight Number | - |
| 5 | date | Date of Survey Flight | yyyymmdd |
| 6 | lat_kkj | Latitude in KKJ | degrees |
| 7 | long_kkj | Longitude in KKJ | degrees |
| 8 | lat_wgs84 | Latitude in WGS84 | degrees |
| 9 | long_wgs84 | Longitude in WGS84 | degrees |
| 10 | x_kkj | Easting (X) in KKJ Finland Uniform Coordinate System | metres |
| 11 | y_kkj | Northing (Y) in KKJ Finland Uniform Coordinate System | metres |
| 12 | x_wgs84 | Easting (X) in WGS84 UTM Zone 35 N | metres |
| 13 | y_wgs84 | Northing (Y) in WGS84 UTM Zone 35 N | metres |
| 14 | gpsz | GPS Elevation (Referenced to Mean Sea Level) | metres |
| 15 | alt_radar | Radar Altimeter | metres |
| 16 | height | Calculated Laser Scanner Clearance (gpsz – dtm) | metres |
| 17 | dtm | Terrain (Referenced to Mean Sea Level) | metres |
| 18 | drape | Planned Drape (Referenced to Mean Sea Level) | metres |
| 19 | diurnal | Magnetic Ground Base Station | nT |
| 20 | mag_raw | Total Magnetic Intensity (Uncompensated) | nT |
| 21 | mag_comp | Total Magnetic Intensity (Compensated) | nT |
| 22 | mag_tmi | Total Magnetic Intensity (Levelled) | nT |
| 23 | igrf | International Geomagnetic Reference Field | nT |
| 24 | mag_rmi | Residual Magnetic Intensity (Levelled) | nT |
| 25 | gD_Equiv_2p67 | Equivalent source derived vertical gravity, terrain correction density 2.67 g/cc | mGal |
| 26 | GDD_Equiv_2p67 | Equivalent source derived vertical gravity gradient, terrain correction density 2.67 g/cc | eötvös |
| 27 | gD_Fourier_2p67 | Fourier derived vertical gravity, terrain correction density 2.67 g/cc, 200m cutoff wavelength | mGal |
| 28 | GDD_Fourier_2p67 | Fourier derived vertical gravity gradient, terrain correction density 2.67 g/cc, 200m cutoff wavelength | eötvös |

**Table 3: Final Aeromagnetic Digital Data** – *ASCII and Geosoft Database Format*

| Variable | Description | Units |
|---|---|---|
| Mosku-Sakatti_TMI | Total Magnetic Intensity | nT |
| Mosku-Sakatti_VD1 | First Vertical Derivative | nT/m |
| Mosku-Sakatti_DTM | Terrain (Referenced to Mean Sea Level) | metres |
| Mosku-Sakatti_DrapeSurface_Equiv | Drape surface for Equivalent Source construction, approximates Fourier Surface | metres |
| Mosku_Sakatt _gD _Equiv_2p67 | Equivalent source derived vertical gravity, terrain correction density 2.67 g/cc | mGal |
| Mosku-Sakatti_gD_Equiv_2p67_conformed | Equivalent source derived vertical gravity, terrain correction density 2.67 g/cc conformed to regional gravity | mGal |
| Mosku-Sakatti_GDD_Equiv_2p67 | Equivalent source derived vertical gravity gradient, terrain correction density 2.67 g/cc | eötvös |
| Mosku-Sakatti_DrapeSurface_Fourier | Drape surface for Fourier reconstruction, smoothed flight surface | metres |
| Mosku-Sakatti_gD_Fourier_0 | Fourier derived vertical gravity, no terrain correction, 200m cutoff wavelength | mGal |
| Mosku-Sakatti_gD_Fourier_2p67 | Fourier derived vertical gravity, terrain correction density 2.67 g/cc, 200m cutoff wavelength | mGal |
| Mosku-Sakatti_gD_Fourier_2p67_conformed | Fourier derived vertical gravity, terrain correction density 2.67 g/cc, 200m cutoff wavelength | mGal |
| Mosku-Sakatti_GDD_Fourier_2p67 | Fourier derived vertical gravity gradient, terrain correction density 2.67 g/cc, 200m cutoff wavelength | eötvös |
| Mosku-Sakatti_GEE_Fourier_2p67 | Fourier derived Gee gradient, terrain correction density 2.67 g/cc, 200m cutoff wavelength | eötvös |
| Mosku-Sakatti_GNN_Fourier_2p67 | Fourier derived Gnn gradient, terrain correction density 2.67 g/cc, 200m cutoff wavelength | eötvös |
| Mosku-Sakatti_GED_Fourier_2p67 | Fourier derived Ged horizontal EW gradient, terrain correction density 2.67 g/cc, 200m cutoff wavelength | eötvös |
| Mosku-Sakatti_GND_Fourier_2p67 | Fourier derived Gnd horizontal NS gradient, terrain correction density 2.67 g/cc, 200m cutoff wavelength | eötvös |
| Mosku-Sakatti_GNE_Fourier_2p67 | Fourier derived Gne curvature gradient, terrain correction density 2.67 g/cc, 200m cutoff wavelength | eötvös |
| Mosku-Sakatti_GUV_Fourier_2p67 | Fourier derived Guv curvature gradient, terrain correction density 2.67 g/cc, 200m cutoff wavelength | eötvös |

**Table 4: Final Aeromagnetic and AGG Grids** – *Geosoft and ERMapper Format*